10 Phonons

In this chapter we will turn our attention to the interaction between light and the phonons in a solid. Phonons are vibrations of the atoms in a crystal lattice, and have resonant frequencies in the infrared spectral region. This contrasts with the optical properties of bound electrons, which occur at visible and ultraviolet frequencies.

The main optical properties of phonons can be explained to a large extent by classical models. We will therefore make extensive use of the classical dipole oscillator model developed in Chapter 2. This will allow us to understand why polar solids reflect and absorb light strongly within a band of infrared frequencies. We will then introduce the concepts of polaritons and polarons, before moving on to discuss the physics of inelastic light scattering. We will see how Raman and Brillouin scattering techniques give us complementary information to infrared reflectivity data, which is why they are so extensively used in phonon physics. Finally we will briefly discuss why phonons have a finite lifetime, and how this affects the reflectivity and inelastic scattering spectra.

We will assume that the reader is familiar with the basic physics of phonons, which is covered in all introductory solid state physics texts. A partial list of suitable preparatory reading is given under Further Reading at the end of the chapter.

10.1 Infrared active phonons

The atoms in a solid are bound to their equilibrium positions by the forces that hold the crystal together. When the atoms are displaced from their equilibrium positions, they experience restoring forces, and vibrate at characteristic frequencies. These vibrational frequencies are determined by the phonon modes of the crystal.

The resonant frequencies of the phonons occur in the infrared spectral region, and the modes that interact directly with light are called **infrared active** (IR active). Detailed selection rules for deciding which phonon modes are IR active can be derived by using group theory. At this level we just discuss the general rules based on the dispersion of the modes, their polarization, and the nature of the bonding in the crystal.

The group theory approach is beyond the scope of this book, although we will give some simple arguments based on symmetry when we consider inelastic light scattering in Section 10.5.

The phonon modes of a crystal are subdivided into two general categories:

- acoustic or optical;
- transverse or longitudinal.

It will come as no surprise to realize that it is the 'optical' rather than the acoustic modes that are directly IR active. These optically active phonons are

able to absorb light at their resonant frequency. The basic process by which a photon is absorbed by the lattice and a phonon is created is represented in Fig. 10.1. Conservation laws require that the photon and the phonon must have the same energy and momentum. We will see below that this condition can only be satisfied for the optical modes.

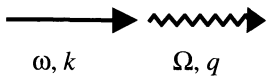

Fig. 10.1 Lattice absorption process by an infrared active phonon. The straight arrow represents the photon that is absorbed, while the wiggly arrow represent the phonon that is created.

Figure 10.2 shows the generic dispersion curves for the acoustic and optical phonons in a simple crystal. The angular frequency Ω of the acoustic and optical phonons is plotted against the wave vector q in the positive half of the first Brillouin zone. At small wave vectors the slope of the acoustic branch is equal to v_s, the velocity of sound in the medium, while the optical modes are essentially dispersionless near $q = 0$.

The figure also shows the dispersion of the light waves in the crystal, which have a constant slope of $v = c/n$, where n is the refractive index. The refractive index has been highly exaggerated here in order to make the dispersion of the photon noticeable on the same scale as the phonon dispersion. The requirement that the photon and phonon should have the same frequency and wave vector is satisfied when the dispersion curves intersect. Since $c/n \gg v_s$, the only intersection point for the acoustic branch occurs at the origin, which corresponds to the response of the crystal to a static electric field. The situation is different for the optical branch: there is an intersection at finite ω, which is identified with the circle in Fig. 10.2. Since the optical branch is essentially flat for small q, the frequency of this resonance is equal to the frequency of the optical mode at $q = 0$.

The phonon dispersion curves for real crystals are more complicated than those shown in Fig. 10.2 because the longitudinal and transverse polarizations tend to have different frequencies.

Electromagnetic waves are transverse, and can only apply driving forces to the transverse vibrations of the crystal. Therefore they can only couple to the transverse optic (TO) phonon modes. This does not mean that we can now completely forget about the longitudinal optic (LO) phonons. As we will see in Section 10.2.2, the LO modes do in fact play an important role in the infrared properties of crystals.

Photons couple to phonons through the driving force exerted on the atoms by the AC electric field of the light wave. This can only happen if the atoms are charged. Therefore, if the atoms are neutral, there will be no coupling to

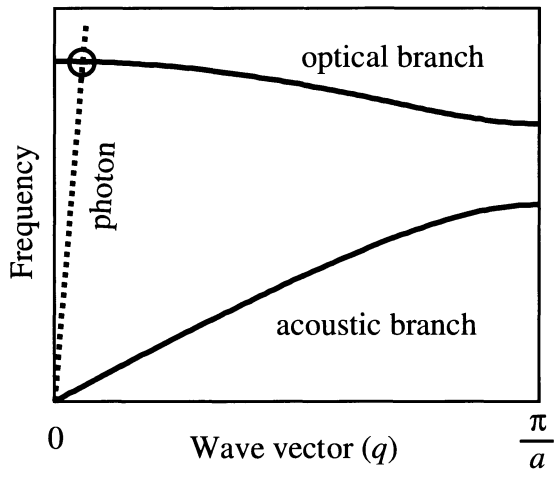

Fig. 10.2 Dispersion curves for the acoustic and optical phonon branches in a typical crystal with a lattice constant of a. The dispersion of the photon modes in the crystal is shown by the dotted line.

the light. This means that the crystal must have some ionic character in order for its TO phonons to be optically active.

The ionicity of a solid arises from the way the crystal binding occurs. An ionic crystal consists of an alternating sequence of positive and negative ions held together by their mutual Coulomb attraction. Covalent crystals, by contrast, consist of neutral atoms with the electrons shared equally between the neighbouring nuclei. This means that none of the optical phonons of purely covalent solids like silicon are IR active. Most other materials fall somewhere between these two limits. For example, the bond in a III–V semiconductor is only partly covalent, and the shared electrons lie slightly closer to the group V atoms than to the group III atoms, which gives the bond a partly ionic character. The bonds with an ionic character are called **polar** bonds to stress the point that the asymmetric electron cloud between the atoms creates a dipole that can interact with electric fields. Provided the bond has some polar character, its phonons can be IR active.

The conclusions of this section are summarized in Table 10.1.

Table 10.1 Infrared activity of the phonon modes in polar and non-polar crystals. LA: longitudinal acoustic, TA: transverse acoustic, LO: longitudinal optic, TA: transverse optic.

Mode	Polar crystal	Non-polar crystal
LA	no	no
TA	no	no
LO	no	no
TO	yes	no

10.2 Infrared reflectivity and absorption in polar solids

Experimental data show that polar solids absorb and reflect light very strongly in the infrared spectral region when the frequency is close to resonance with the TO phonon modes. We have come across several examples of this already. For example, the transmission spectra of sapphire and CdSe given in Fig. 1.4 show that there are spectral regions in the infrared where no light is transmitted. This is a consequence of lattice absorption.

The aim of this section is to account for this result by modelling the interaction of photons with TO phonons. To do this we will make extensive use of the classical oscillator model developed in Chapter 2, especially Section 2.2. This will allow us to calculate the frequency dependence of the complex dielectric constant $\tilde{\epsilon}_r(\omega)$, from which we will be able to determine the important optical properties such as the reflectivity and absorption.

10.2.1 The classical oscillator model

The interaction between electromagnetic waves and a TO phonon in an ionic crystal is most easily treated by considering a linear chain, as illustrated in Fig. 10.3. The chain consists of a series of unit cells, each containing a positive ion (black circle) and a negative ion (grey circle). The waves are taken to be propagating along the chain in the z direction. We are dealing with a transverse mode, and so the displacement of the atoms is in the x or y directions. Furthermore, in an optic mode the different atoms within each unit cell move in opposite directions, with a fixed ratio between their displacements which is not necessarily equal to unity.

LO modes do not interact with light because the displacement of the atoms generates a longitudinal electric field, which is perpendicular to that of the light wave.

We are interested in the interaction between a TO phonon mode with $q \approx 0$ and an infrared light wave of the same frequency and wave vector. This means that we are considering phonons with a very long wavelength of $\sim 10\ \mu$m matched to that of an infrared photon. This phonon wavelength is huge

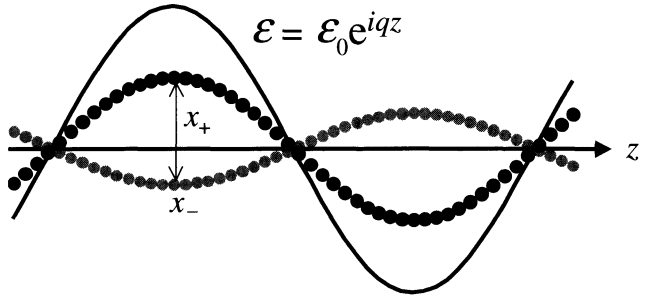

Fig. 10.3 Interaction of a TO phonon mode propagating in the z direction with an electromagnetic wave of the same wave vector. The black circles represent positive ions, while the grey circles represent the negative ions. The solid line represents the spatial dependence of the electric field of the electromagnetic wave.

compared to the size of a unit cell in a crystal, which is usually less than 10^{-9}m. The size of the atoms has been highly exaggerated in Fig. 10.3 to make the physics of the interaction clearer. In fact, the real size of the atoms is tiny compared to the wavelength, and there will be thousands of unit cells within one period of the wave.

The solid line in the figure represents the spatial dependence of the AC electric field of the infrared light wave. At resonance, the wave vector of the photon and the phonon are the same. This means that the driving force exerted by the light on the positive and negative ions is in phase with the lattice vibration. At the same time, the antiparallel displacements of the oppositely charged atoms generate an AC electric field in phase with the external light. This implies that there is a strong interaction between the TO phonon mode and the light wave when the wave vectors and frequencies match.

For long wavelength TO modes with $q \approx 0$, the motion of the atoms in different unit cells is almost identical, and we therefore need to concentrate on what is happening within the unit cell itself. This enables us to see that there is a close connection between the TO phonons at $q = 0$ and the vibrational modes of the molecules from which the crystal is formed. We can therefore make use of some of the principles developed in molecular physics, for example: the selection rules for deciding whether a particular phonon mode is IR or Raman active. (cf. Section 10.5.2.)

The data for SiO_2 glass shown in Fig. 2.7 illustrates the connection between the infrared absorption in solids and that of the constituent molecules quite well. The glass is amorphous, and therefore does not have long range order with delocalized phonon modes. The absorption in the range 10^{13}–10^{14}Hz is basically caused by the vibrational absorption of the SiO_2 molecules themselves, although the frequencies are not necessarily exactly the same in the solid as in the free molecule.

The interaction between the TO phonon and the light wave can be modelled by writing down the equations of motion for the displaced ions. The displacements of the positive and negative ions in a TO mode are in opposite directions and are given the symbols x_+ and x_- respectively, as indicated in Fig. 10.3. The appropriate equations of motion are:

$$m_+ \frac{d^2 x_+}{dt^2} = -K(x_+ - x_-) + \mathsf{q}\mathcal{E}(t) \tag{10.1}$$

$$m_- \frac{d^2 x_-}{dt^2} = -K(x_- - x_+) - \mathsf{q}\mathcal{E}(t) \tag{10.2}$$

where m_+ and m_- are the masses of the two ions, K is the restoring constant of the medium, and $\mathcal{E}(t)$ is the external electric field due to the light wave. The effective charge per ion is taken to be $\pm\mathsf{q}$.

For a strongly ionic crystal such as NaCl, q would just be equal to $\pm e$. However, for crystals with polar covalent bonds such as the III–V compounds, q will represent an effective charge which is determined by the asymmetry of the electron cloud within the bond.

By dividing eqn 10.1 by m_+ and eqn 10.2 by m_-, and then subtracting, we obtain:

$$\frac{d^2}{dt^2}(x_+ - x_-) = -\frac{K}{\mu}(x_+ - x_-) + \frac{\mathsf{q}}{\mu}\mathcal{E}(t)\,, \tag{10.3}$$

where μ is the reduced mass given by

$$\frac{1}{\mu} = \frac{1}{m_+} + \frac{1}{m_-}. \tag{10.4}$$

By putting $x = x_+ - x_-$ for the relative displacement of the positive and negative ions within their unit cell, we can recast eqn 10.3 in the simpler form:

$$\frac{d^2x}{dt^2} + \Omega_{\mathrm{TO}}^2 x = \frac{\mathsf{q}}{\mu}\mathcal{E}(t), \tag{10.5}$$

where we have written Ω_{TO}^2 for K/μ. Ω_{TO} represents the natural vibrational frequency of the TO mode at $q = 0$ in the absence of the external light field.

Equation 10.5 represents the equation of motion for undamped oscillations of the lattice driven by the forces exerted by the AC electric field of the light wave. In reality, we should have incorporated a damping term to account for the finite lifetime of the phonon modes. The physical significance of the phonon lifetime will be discussed further in Section 10.6. At this stage, we simply introduce a phenomenological damping rate γ, and rewrite eqn 10.5 as

$$\frac{d^2x}{dt^2} + \gamma\frac{dx}{dt} + \Omega_{\mathrm{TO}}^2 x = \frac{\mathsf{q}}{\mu}\mathcal{E}(t). \tag{10.6}$$

This now represents the response of a damped TO phonon mode to a resonant light wave.

Equation 10.6 is identical in form to eqn 2.5 in Chapter 2, with m_0 replaced by μ, ω_0 by Ω_{TO} and $-e$ by q. Therefore, we can use all the results derived in Section 2.2 to model the response of the medium to a light field of angular frequency ω with $\mathcal{E}(t) = \mathcal{E}_0 e^{i\omega t}$. In particular, we can go directly to the formula for the frequency dependence of the dielectric constant without repeating all the steps in the derivation. By adapting the symbols appropriately in eqn 2.14, we immediately write down:

$$\epsilon_{\mathrm{r}}(\omega) = 1 + \chi + \frac{N\mathsf{q}^2}{\epsilon_0\mu}\frac{1}{\left(\Omega_{\mathrm{TO}}^2 - \omega^2 - i\gamma\omega\right)}, \tag{10.7}$$

where $\epsilon_{\mathrm{r}}(\omega)$ is the complex dielectric constant at angular frequency ω. χ represents the non-resonant susceptibility of the medium, and N is the number of unit cells per unit volume.

Equation 10.7 can be tidied up by introducing the static and high frequency dielectric constants ϵ_{st} and ϵ_∞ respectively. In the limits of low and high frequency, we obtain from eqn 10.7:

$$\epsilon_{\mathrm{st}} \equiv \epsilon_{\mathrm{r}}(0) = 1 + \chi + \frac{N\mathsf{q}^2}{\epsilon_0\mu\Omega_{\mathrm{TO}}^2}, \tag{10.8}$$

and

$$\epsilon_\infty \equiv \epsilon_{\mathrm{r}}(\infty) = 1 + \chi. \tag{10.9}$$

Thus we can write:

$$\epsilon_{\mathrm{r}}(\omega) = \epsilon_\infty + (\epsilon_{\mathrm{st}} - \epsilon_\infty)\frac{\Omega_{\mathrm{TO}}^2}{\left(\Omega_{\mathrm{TO}}^2 - \omega^2 - i\gamma\omega\right)}. \tag{10.10}$$

In principle, we should consider the local field corrections discussed in Section 2.2.4 here. This is an unnecessary complication at this level which does not add much to the main conclusions. We will therefore neglect local field effects, and base our discussion on eqn 10.10.

This is our main result, which will be used in the next subsections to derive the infrared optical coefficients. As discussed in Section 2.2.2, and in particular in connection with Fig. 2.6, we should understand '$\omega = \infty$' in a relative sense here. ϵ_∞ represents the dielectric constant at frequencies well above the phonon resonance, but below the next natural frequency of the crystal due, for example, to the bound electronic transitions in the visible/ultraviolet spectral region.

10.2.2 The Lyddane–Sachs–Teller relationship

Before working out the frequency dependence of the infrared reflectivity, it is useful to investigate one rather striking implication of eqn 10.10. Suppose we have a lightly damped system so that we can set $\gamma = 0$. Then at a certain frequency which we label ω', eqn 10.10 tells us that the dielectric constant can fall to zero. The condition for this to happen is:

$$\epsilon_r(\omega') = 0 = \epsilon_\infty + (\epsilon_{st} - \epsilon_\infty)\frac{\Omega_{TO}^2}{\left(\Omega_{TO}^2 - \omega'^2\right)}. \tag{10.11}$$

This can be solved to obtain:

$$\omega' = \left(\frac{\epsilon_{st}}{\epsilon_\infty}\right)^{\frac{1}{2}} \Omega_{TO}. \tag{10.12}$$

What does $\epsilon_r = 0$ mean physically ? In a medium with no free charges, the total charge density will be zero. Hence Gauss's law (eqn A.10) tells us that

$$\nabla \cdot \mathbf{D} = \nabla \cdot (\epsilon_r \epsilon_0 \boldsymbol{\mathcal{E}}) = 0, \tag{10.13}$$

where we have made use of eqn A.3 to relate the electric displacement $\mathbf{D}$ to the electric field $\boldsymbol{\mathcal{E}}$ in a dielectric medium. When we consider the propagation of electromagnetic waves through the dielectric, we look for wave solutions of the form:

$$\boldsymbol{\mathcal{E}}(\mathbf{r}, t) = \boldsymbol{\mathcal{E}}_0 \, e^{i(\mathbf{k}\cdot\mathbf{r} - \omega t)}. \tag{10.14}$$

On substituting eqn 10.14 into eqn 10.13, we usually assume that $\epsilon_r \neq 0$ and therefore conclude that $\mathbf{k} \cdot \boldsymbol{\mathcal{E}} = 0$. This tells us that the electric field must be perpendicular to the direction of the wave and therefore that the waves are transverse. However, if $\epsilon_r = 0$, we can satisfy eqn 10.13 with waves in which $\mathbf{k} \cdot \boldsymbol{\mathcal{E}} \neq 0$, that is, with longitudinal waves. Thus we conclude that the dielectric can support longitudinal electric field waves at frequencies which satisfy $\epsilon_r(\omega) = 0$.

In the same way that TO phonon modes generate a transverse electric field wave, the LO phonon modes generate a longitudinal electric field wave. Thus the waves at $\omega = \omega'$ correspond to LO phonon waves, and we identify ω' with the frequency of the LO mode at $q = 0$, namely Ω_{LO}. This allows us to rewrite eqn 10.12 in the following form:

$$\frac{\Omega_{LO}^2}{\Omega_{TO}^2} = \frac{\epsilon_{st}}{\epsilon_\infty}. \tag{10.15}$$

We came across another situation in which ϵ_r is zero when we discussed plasmons in Section 7.5. We saw there that the plasma oscillations that cause ϵ_r to be zero also correspond to longitudinal electric field waves.

Table 10.2 Comparison of the measured ratio Ω_{LO}/Ω_{TO} for several materials to the value predicted by the Lyddane–Sachs–Teller relationship. After [1].

Crystal	Ω_{LO}/Ω_{TO}	$(\epsilon_{st}/\epsilon_\infty)^{\frac{1}{2}}$
Si	1	1
GaAs	1.07	1.08
AlAs	1.12	1.11
BN	1.24	1.26
ZnSe	1.19	1.19
MgO	1.81	1.83
AgF	1.88	1.88

This result is known as the **Lyddane–Sachs–Teller (LST) relationship**. The validity of the relationship can be checked by comparing the values of Ω_{LO}/Ω_{TO} deduced from neutron or Raman scattering experiments with those calculated from eqn 10.15 using known values of the dielectric constants. Some results are given in Table 10.2. It is apparent that the agreement is generally very good.

An interesting corollary of the LST relationship is that it implies that the LO phonon and TO phonon modes of non-polar crystals are degenerate. This follows because there is no infrared resonance, and therefore $\epsilon_{st} = \epsilon_\infty$. This is indeed the case for the purely covalent crystals of the group IV elements, namely diamond (C), silicon and germanium.

10.2.3 Restrahlen

Having discussed the properties of the system at the special frequency of $\omega = \Omega_{LO}$, we can now calculate the infrared optical constants. It is easier to understand the general behaviour if we assume that the damping term is small. We thus set $\gamma = 0$ in eqn 10.10, and discuss the properties of a material with a dielectric constant that has the following frequency dependence:

$$\epsilon_r(\nu) = \epsilon_\infty + (\epsilon_{st} - \epsilon_\infty)\frac{\nu_{TO}^2}{(\nu_{TO}^2 - \nu^2)}. \tag{10.16}$$

We have divided all the angular frequencies by 2π here, so that we can compare the predictions to experimental data, which are usually presented against frequency (ν) rather than angular frequency (ω). We will discuss the effect of including the damping term when we compare our model to the experimental data in connection with Fig. 10.5.

Figure 10.4(a) plots the frequency dependence of the dielectric constant $\epsilon_r(\nu)$ calculated from eqn 10.16 for a polar crystal with the following parameters: $\nu_{TO} = 10$ THz, $\nu_{LO} = 11$ THz, $\epsilon_{st} = 12.1$ and $\epsilon_\infty = 10$. These figures are quite close to those that would be found in a typical III–V semiconductor. Note that the phonon frequencies have been chosen to satisfy the LST relationship given in eqn 10.15.

1 THz = 10^{12} Hz

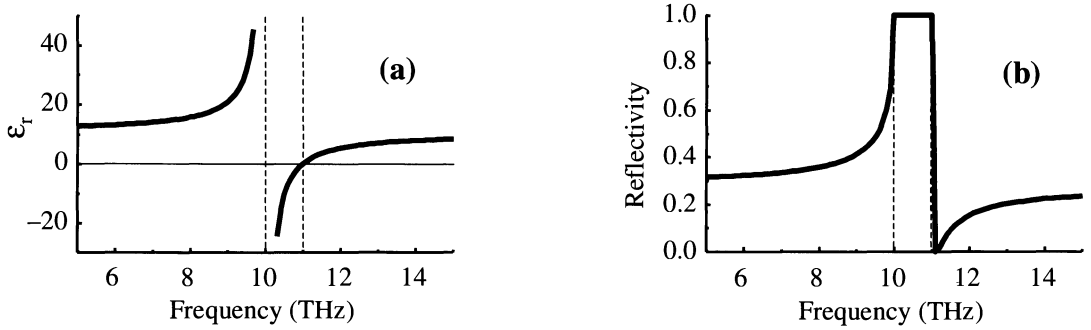

Fig. 10.4 Frequency dependence of the dielectric constant and reflectivity for a crystal with $\nu_{TO} = 10$ THz, $\nu_{LO} = 11$ THz, $\epsilon_{st} = 12.1$ and $\epsilon_\infty = 10$. The curves have been calculated from eqns 10.16 and 10.17. Phonon damping is ignored in this calculation.

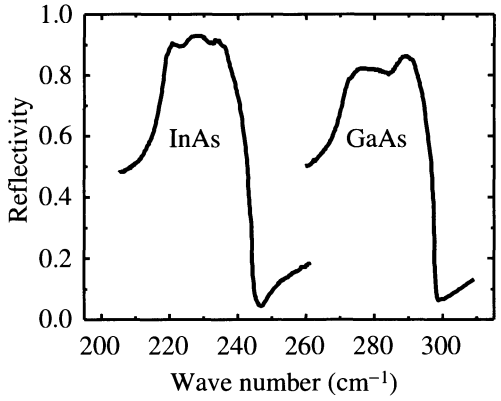

Fig. 10.5 Infrared reflectivity of InAs and GaAs at 4.2 K. A wave number of 1 cm^{-1} is equivalent to a frequency of 2.998×10^{10} Hz. After [2], copyright © 1967 by Academic Press, reproduced by permission of the publisher.

At low frequencies the dielectric constant is just equal to ϵ_{st}. As ν increases from 0, $\epsilon_r(\nu)$ gradually increases until it diverges when the resonance at ν_{TO} is reached. Between ν_{TO} and ν_{LO}, ϵ_r is negative. Precisely at $\nu = \nu_{LO}$, $\epsilon_r = 0$. Thereafter, ϵ_r is positive, and gradually increases asymptotically towards the value of ϵ_∞.

The most important optical property of a polar solid in the infrared spectral region is the reflectivity. This can be calculated from the dielectric constant using eqn 1.26:

$$R = \left|\frac{\tilde{n}-1}{\tilde{n}+1}\right|^2 = \left|\frac{\sqrt{\epsilon_r}-1}{\sqrt{\epsilon_r}+1}\right|^2. \qquad (10.17)$$

We can see from eqn 1.17 that $\sqrt{\epsilon_\infty}$ corresponds to the refractive index of the medium at frequencies well above the optical phonon resonances. This will be the refractive index measured at near-infrared and visible frequencies the below band gap of the material.

Figure 10.4(b) plots the reflectivity calculated using eqn 10.17 for the dielectric constant shown in Fig. 10.4(a). At low frequencies the reflectivity is $(\sqrt{\epsilon_{st}}-1)^2/(\sqrt{\epsilon_{st}}+1)^2$. As ν approaches ν_{TO}, R increases towards unity. In the frequency region between ν_{TO} and ν_{LO}, $\sqrt{\epsilon_r}$ is imaginary, so that R remains equal to unity. R drops rapidly to zero as ν increases above ν_{LO} (see Exercise 10.2), and then increases gradually towards the high frequency asymptote of $(\sqrt{\epsilon_\infty}-1)^2/(\sqrt{\epsilon_\infty}+1)^2$.

We see from this analysis that the reflectivity is equal to 100 % in the frequency region between ν_{TO} and ν_{LO}. This frequency region is called the **restrahlen** band. Restrahlen is the German word for 'residual rays'. Light cannot propagate into the medium in the restrahlen band.

Figure 10.5 shows experimental data for the reflectivity of InAs and GaAs in the infrared spectral region. InAs has TO and LO phonon frequencies at 218.9 cm^{-1} and 243.3 cm^{-1} respectively, while for GaAs we have $\nu_{TO} = 273.3\,\text{cm}^{-1}$ and $\nu_{LO} = 297.3\,\text{cm}^{-1}$. We see that the reflectivity is very high for frequencies between the TO and LO phonon frequencies in both materials, and there is a sharp dip in the reflectivity just above the LO phonon resonance.

Experimental infrared spectra are frequently plotted against the wave number $\bar{\nu} \equiv 1/\lambda$. The wave number is effectively a frequency unit, with 1 cm^{-1} equivalent to 2.998×10^{10} Hz.

On comparing these results with the prediction shown in Fig. 10.4(b), we see that the general agreement between the model and the experimental data is very good. The main difference is that in both materials the maximum reflectivity in the restrahlen band is less than 100 %. This reduction in the reflectivity is caused by ignoring the damping term. (See Example 10.1 and Exercise 10.4.) The damping also broadens the edge so that there is only a minimum in R just above ν_{LO} rather than a zero.

The magnitude of γ can be found by fitting the experimental data to the full dependence given in eqn 10.10. The values of γ obtained in this way are around 10^{11}–10^{12} s^{-1}, which implies that the optical phonons have a lifetime of about 1–10 ps. The physical significance of this short lifetime will be discussed in Section 10.6.

$1\,ps = 10^{-12}\,s.$

10.2.4 Lattice absorption

When we introduced the classical oscillator model in Section 2.2 of Chapter 2, we made the point that we expect high absorption coefficients whenever the frequency matches the natural resonances of the medium. The reader might therefore be wondering why we have been concentrating on calculating the reflectivity rather than the absorption due to the TO phonon resonances.

This question is further prompted by recalling the analogy between the infrared absorption of polar solids and that of isolated molecules. In both cases we are basically treating the interaction of photons with quantized vibrational modes. In molecular physics we usually discuss this in terms of the infrared absorption spectrum. The absorption spectra show strong peaks whenever the frequency coincides with the infrared active vibrational modes and the molecule can absorb a photon by creating one vibrational quantum. This is directly analogous to the process for solids shown in Fig. 10.1 in which a photon is absorbed and a phonon is created.

The answer to these questions is that the lattice does indeed absorb very strongly whenever the photon is close to resonance with the TO phonon. As stressed in Chapter 2, the fundamental optical properties of a dielectric – the absorption, refraction and reflectivity – are all related to each other because they are all determined by the complex dielectric constant. The distinction between absorption and reflection is merely a practical one. Polar solids have such high absorption coefficients in the infrared that unless the crystal is less than $\sim$ 1 μm thick, no light at all will be transmitted. This is clearly seen in the transmission spectra of Al_2O_3 and CdSe shown in Fig. 1.4. For this reason, it is only sensible to consider lattice absorption in thin film samples. In thick crystals, we must use reflectivity measurements to determine the vibrational frequencies. This contrasts with molecular physics, where we are usually dealing with low density gases, which give rise to much smaller absorption coefficients.

The absorption coefficients expected at the resonance with the TO phonon can be calculated from the imaginary part of the dielectric constant. At $\omega = \Omega_{TO}$ we have from eqn 10.10:

$$\epsilon_r(\Omega_{TO}) = \epsilon_\infty + i(\epsilon_{st} - \epsilon_\infty)\frac{\Omega_{TO}}{\gamma}\,. \tag{10.18}$$

The extinction coefficient κ can be worked out from ϵ_r using eqn 1.23, and then the absorption coefficient α can be determined from κ using eqn 1.16. Typical values for α are in the range 10^6–10^7 m^{-1}. (See Example 10.1 and Exercise 10.6.) This is why the sample must be thinner than $\sim$ 1 μm in order to perform practical absorption measurements. Infrared absorption measurements on thin film samples do indeed confirm that the absorption is very high at the TO phonon resonance frequency.

Example 10.1

The static and high frequency dielectric constants of NaCl are $\epsilon_{st} = 5.9$ and $\epsilon_\infty = 2.25$ respectively, and the TO phonon frequency ν_{TO} is 4.9 THz.

(i) Calculate the upper and lower wavelengths of the restrahlen band.

(ii) Estimate the reflectivity at 50 μm, if the damping constant γ of the phonons is $10^{12}\,s^{-1}$.

(iii) Calculate the absorption coefficient at 50 μm.

Solution

(i) The restrahlen band runs from ν_{TO} to ν_{LO}. We are given ν_{TO}, and we can calculate ν_{LO} from the LST relationship (eqn 10.15). This gives

$$\nu_{LO} = \left(\frac{\epsilon_{st}}{\epsilon_\infty}\right)^{\frac{1}{2}} \times \nu_{TO} = \left(\frac{5.9}{2.25}\right)^{\frac{1}{2}} \times 4.9\,\text{THz} = 7.9\,\text{THz}.$$

Therefore the restrahlen band runs from 4.9 THz to 7.9 THz, or 38 μm to 61 μm.

(ii) At 50 μm we are in middle of the restrahlen band. We therefore expect the reflectivity to be high. We insert the values for ϵ_{st}, ϵ_∞, γ and $\Omega_{TO} = 2\pi\nu_{TO}$ into eqn 10.10 with $\omega = 2\pi\nu$ ($\nu = 6$ THz) to find:

$$\epsilon_r = 2.25 + 3.65\frac{(4.9)^2}{(4.9)^2 - 6^2 - i(1)(6)/2\pi} = -5.0 + 0.57i\,.$$

We then obtain the real and imaginary parts of the refractive index from eqns 1.22 and 1.23:

$$n = \frac{1}{\sqrt{2}}\left(-5.0 + [(-5.0)^2 + (0.57)^2]^{\frac{1}{2}}\right)^{\frac{1}{2}} = 0.13\,,$$

and

$$\kappa = \frac{1}{\sqrt{2}}\left(+5.0 + [(-5.0)^2 + (0.57)^2]^{\frac{1}{2}}\right)^{\frac{1}{2}} = 2.2.$$

We finally substitute these values of n and κ into eqn 1.26 to find the reflectivity:

$$R = \frac{(n-1)^2 + \kappa^2}{(n+1)^2 + \kappa^2} = \frac{(-0.87)^2 + (2.2)^2}{(1.13)^2 + (2.2)^2} = 0.91.$$

This value is close to the measured reflectivity of NaCl in the restrahlen band at room temperature.

(iii) We can calculate the absorption coefficient α from the extinction coefficient using eqn 1.16. We have already worked out that $\kappa = 2.2$ in part (ii). Hence we find:

$$\alpha = \frac{4\pi\kappa}{\lambda} = \frac{4\pi \times 2.2}{50 \times 10^{-6}} = 5.5 \times 10^5\,\text{m}^{-1}\,.$$

This shows that the light would be absorbed in a thickness of about 2 μm.

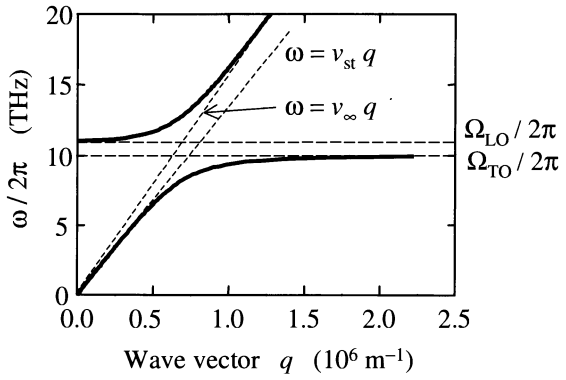

Fig. 10.6 Polariton dispersion predicted from eqn 10.19 with ϵ_r given by eqn 10.16. The curves are calculated for a crystal with ν_{TO} = 10 THz, ϵ_{st} = 12.1 and ϵ_∞ = 10. The asymptotic velocities v_{st} and v_∞ are equal to $c/\sqrt{\epsilon_{st}}$ and $c/\sqrt{\epsilon_\infty}$ respectively.

10.3 Polaritons

The dispersion curves of the photons and TO phonons were discussed in broad terms in connection with Fig. 10.2. We now wish to consider the circled intersection point in Fig. 10.2 in more detail. As we will see, the two dispersion curves do not actually cross each other. This is a consequence of the strong coupling between the TO phonons and the photons when their frequencies and wave vectors match. This leads to the characteristic anticrossing behaviour which is observed in many coupled systems.

The coupled phonon–photon waves are called **polaritons**. As the name suggests, these classical waves are mixed modes which have characteristics of both polarization waves (the TO phonons) and the photons. The dispersion of the polaritons can be deduced from the relationship:

$$\omega = vq = \frac{c}{\sqrt{\epsilon_r}} q \,, \tag{10.19}$$

where the second part of the equation comes from eqn A.29, with $\mu_r = 1$. The resonant response of the polar solid is contained implicity in the frequency dependence of ϵ_r.

Figure 10.6 shows the polariton dispersion calculated for a lightly damped medium. The dielectric constant is given by eqn 10.16, and is plotted for the same parameters as in Fig. 10.4(a). At low frequencies the dielectric constant is equal to ϵ_{st}, and the dispersion of the modes is given by $\omega = cq/\sqrt{\epsilon_{st}}$. As ω approaches Ω_{TO}, the dielectric constant increases, and the velocity of the waves decreases, approaching zero at Ω_{TO} itself. For frequencies in the restrahlen band between Ω_{TO} and Ω_{LO}, the dielectric constant is negative. No modes can propagate, and all the photons that are incident on the medium are reflected. For frequencies above Ω_{LO}, ϵ_r is positive again and propagating modes are possible once more. The velocity of the waves gradually increases with increasing frequency, approaching a value of $c/\sqrt{\epsilon_\infty}$ at high frequencies.

The dispersion of the polariton modes has been measured for a number of materials. Figure 10.7 shows the measured dispersion of the TO phonons and LO phonons in GaP at small wave vectors. The results were obtained by Raman scattering techniques. (See Section 10.5.2.) The experimental data reproduce very well the polariton dispersion model indicated in Fig. 10.6. The solid line

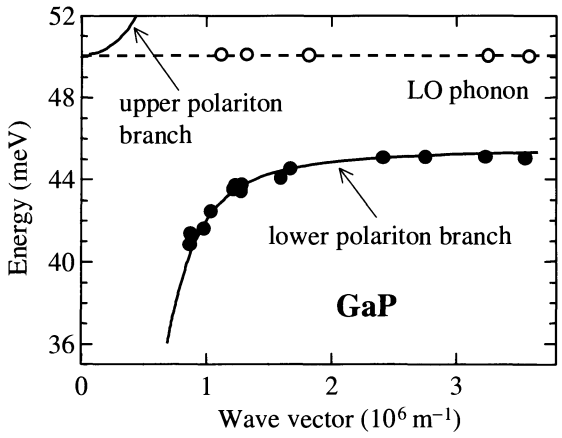

Fig. 10.7 Dispersion of the TO and LO phonons in GaP measured by Raman scattering. The solid lines are the predictions of the polariton model with $h\nu_{TO} = 45.5$ meV, $\epsilon_\infty = 9.1$ and $\epsilon_{st} = 11.0$. After [3], copyright 1965 American Institute of Physics, reprinted with permission.

is the calculated polariton dispersion, which gives a very accurate fit to the experimental points. Note that the LO phonons do not show any dispersion here because they do not couple to the light waves.

10.4 Polarons

So far in this chapter we have been considering the direct interaction between a light wave and the phonons in a crystal. As we have seen, this gives rise to strong absorption and reflection in the infrared spectral region. The optical phonons can, however, contribute indirectly to a whole host of other optical properties that depend primarily on the electrons through the **electron–phonon coupling**. In this section we will consider the **polaron** effect, which is one of the most important examples of this.

Consider the motion of a free electron through a polar solid, as shown in Fig. 10.4. The electron will attract the positive ions that are close to it, and repel the negative ones. This produces a local displacement of the lattice in the immediate vicinity of the electron. The lattice distortion accompanies the electron as it moves through the crystal. The electron with its local lattice

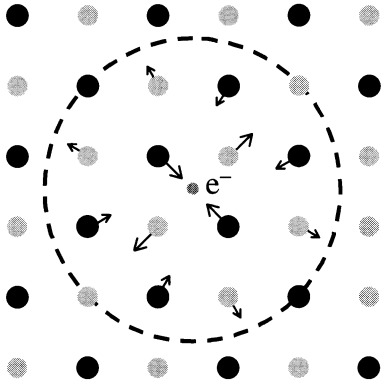

Fig. 10.8 Schematic representation of a polaron. A free electron moving through an ionic lattice attracts the positive (black) ions, and repels the negative (grey) ones. This produces a local distortion of the lattice within the polaron radius shown by the dashed circle

distortion is equivalent to a new elementary excitation of the crystal, and is called a polaron.

The polaron effect can be conceived in terms of an electron surrounded by a cloud of virtual phonons. We think of the electron absorbing and emitting phonons as it moves through the crystal. These phonons produce the local lattice distortion. The displacement of the ions is in the same direction as the electric field of the electron, we are therefore dealing with longitudinal optic phonons.

The strength of the electron–phonon interaction in a polar solid can be quantified by the dimensionless coupling constant α_{ep}, which is given by:

$$\alpha_{ep} = \frac{1}{137}\left(\frac{m^* c^2}{2\hbar\Omega_{LO}}\right)^{\frac{1}{2}}\left[\frac{1}{\epsilon_\infty} - \frac{1}{\epsilon_{st}}\right], \tag{10.20}$$

where $1/137$ is the fine structure constant from atomic physics. The mass m^* that appears here is the usual effective mass deduced from the curvature of the band structure (c.f. eqn C.6):

$$m^* = \hbar^2\left(\frac{d^2E}{dk^2}\right)^{-1}. \tag{10.21}$$

Values for α_{ep} for three binary compound semiconductors, namely GaAs, ZnSe and AgCl, are given in Table 10.3. We see that the coupling constant increases from GaAs (0.06) through ZnSe (0.40) to AgCl (2.2). This is because the ionicity increases as we go from the III–V semiconductor, in which the bonding is predominantly covalent, to the I–VII compound, which is highly ionic.

This effective mass given by eqn 10.21 is calculated by assuming that the lattice is rigid. However, the concept of a rigid lattice is only a theoretical one, and any experiment we perform to measure m^* will actually measure the polaron mass m^{**} instead. This is because it is not possible to hold the lattice rigid as the electron moves. The polaron mass is larger than the rigid lattice mass because the electron has to drag the local lattice distortion with it as it moves.

An example of an experiment to measure the effective mass is **cyclotron resonance**. In this technique, we measure the infrared absorption in the presence of a magnetic field B. As discussed in Section 3.3.6, the electron energy is quantized in terms of the cyclotron energy:

$$E_n = (n + \tfrac{1}{2})\hbar\omega_c, \tag{10.22}$$

where n is an integer, and

$$\omega_c = \frac{eB}{m^*}. \tag{10.23}$$

Optical transitions with $\Delta n = \pm 1$ can take place between the ladder of levels defined by eqn 10.22. We therefore observe absorption at a wavelength λ given by:

$$\frac{hc}{\lambda} = \frac{e\hbar B}{m^*}. \tag{10.24}$$

This absorption usually occurs in the far-infrared spectral region, and the effective mass can be deduced from the values of λ and B at resonance. In a

It can be shown that the average number of virtual LO phonons that move with the electron is equal to $\alpha_{ep}/2$. We do not consider the longitudinal acoustic modes here because they do not produce a polarization in the medium: the positive and negative ions move in the same direction, and this produces no electric dipole moment.

The polaron theory can be applied equally to electrons or holes by taking the appropriate effective masses in the formulæ. In a non-polar crystal such as silicon, $\epsilon_\infty = \epsilon_{st}$, and $\alpha_{ep} = 0$. There is therefore no polaron effect.

Table 10.3 Electron-phonon coupling constant α_{ep} calculated from eqn 10.20 for GaAs, ZnSe, and AgCl. The figures for ZnSe are for the cubic crystal structure. After [1].

	GaAs	ZnSe	AgCl
m_e^*/m_0	0.067	0.13	0.30
ϵ_∞	10.9	5.4	3.9
ϵ_{st}	12.4	7.6	11.1
Ω_{LO} (THz)	53.7	47.7	36.9
α_{ep}	0.06	0.40	2.2

typical experiment, we use a fixed wavelength source from an infrared laser and find the value of B which gives the maximum absorption. For example, the cyclotron resonance occurs at about 6.1 T in GaAs ($m^* = 0.067m_0$) for the 118 μm line from a methanol laser. The effective mass we find this way is the polaron mass m^{**}, not the value determined by the curvature of the bands given by eqn 10.21.

A particularly clear manifestation of the electron–phonon coupling can be observed in cyclotron resonance experiments when $B = m^*\Omega_{LO}/e$, so that $\omega_c = \Omega_{LO}$. The degenerate electron and phonon modes anticross with each other as the field is swept through this condition, and the cyclotron resonance line splits into a doublet. The magnitude of the splitting is directly proportional to the electron–phonon coupling constant α_{ep}. This effect was first observed in n-type InSb.

If the electron–phonon coupling constant α_{ep} is small, we can give an explicit relationship between the rigid lattice effective mass m^* and the polaron mass m^{**}:

$$\frac{m^{**}}{m^*} = \frac{1}{1 - \alpha_{ep}/6} \approx 1 + \frac{1}{6}\alpha_{ep} . \tag{10.25}$$

Values of m^* are actually worked from the measured values of m^{**} by applying eqn 10.25. For III–V semiconductors like GaAs with $\alpha_{ep} < 0.1$, m^{**} only differs from m^* by about 1 %. The polaron effect is thus only a small correction. This correction becomes more significant for II–VI compounds (e.g. $\sim$ 7 % for ZnSe). With highly ionic crystals like AgCl, the small α_{ep} approximation is not valid. The actual polaron mass of AgCl is 0.43, which is about 50 % larger than the rigid lattice value.

It can be shown that, in addition to the change of the mass, the polaron effect causes a reduction in the band gap by an amount:

$$\Delta E_g = -\alpha_{ep}\hbar\Omega_{LO} . \tag{10.26}$$

With a III–V material like GaAs, this again produces only a relatively small effect: $\Delta E_g \sim -0.1$ %. In practice, when we measure E_g by optical spectroscopy we always measure the polaron value.

Another important parameter of the polaron is its radius, r_p, which specifies how far the lattice distortion extends. This is depicted schematically in Fig. 10.4 by the dashed circle drawn around the electron that causes the lattice distortion. If α_{ep} is small, we can give an explicit formula for r_p:

$$r_p = \left(\frac{\hbar}{2m^*\Omega_{LO}}\right)^{\frac{1}{2}} . \tag{10.27}$$

This gives $r_p = 4.0$ nm for GaAs and 3.1 nm for ZnSe. Both values are significantly larger than the unit cell size ($\sim$ 0.5 nm), which is important because the theory used to derive eqns 10.25–10.27 assumes that we can treat the medium as a polarizable continuum. This approximation is only valid if the radius of the polaron is very much greater than the unit cell size. A polaron which satisfies this criterion is called a **large polaron**. In highly ionic solids such as AgCl and the alkali halides, α_{ep} is not small and the polaron radius is comparable to the unit cell size. In this case we have a **small polaron**. The mass and radius have to be calculated from first principles.

The small polaron effect in highly ionic crystals leads to **self-trapping** of the charge carriers. The local lattice distortion is very strong, and the charge carrier can get completely trapped in its own lattice distortion. The carrier effectively digs itself into a pit and cannot get out of it. This is particularly the case for the holes in alkali halide crystals. The only way they can move is by **hopping** to a new site. The electrical conductivity of most alkali halide crystals is limited by this thermally activated hopping process at room temperature.

Polaronic hopping effects are also important in the conduction processes in organic semiconductors like polydiacetylene.

Self-trapping effects are important in determining the energies of Frenkel excitons. As discussed in Section 4.5, these are bound electron–hole pairs localized at individual atom or molecule sites within the lattice. The self-trapping of either the electron or hole can exacerbate the tendency for the exciton to localize, thereby instigating the transition from Wannier (free) to Frenkel exciton behaviour. The ground state excitons observed in many alkali halide, rare gas and organic crystals are of the self-trapped Frenkel type.

10.5 Inelastic light scattering

Inelastic light scattering describes the phenomenon by which a light beam is scattered by an optical medium and changes its frequency in the process. It contrasts with elastic light scattering, in which the frequency of the light is unchanged. The interaction process is illustrated in Fig. 10.9. Light incident with angular frequency ω_1 and wave vector $\mathbf{k}_1$ is scattered by an excitation of the medium of frequency Ω and wave vector $\mathbf{q}$. The scattered photon has frequency ω_2 and wave vector $\mathbf{k}_2$. Inelastic light scattering can be mediated by many different types of elementary excitations in a crystal, such as phonons, magnons or plasmons. In this chapter we will be concerned exclusively with phonon processes.

We presented a Raman scattering spectrum from plasmons in n-type GaAs in Fig. 7.13.

Inelastic light scattering from phonons is generally subdivided as to whether it is the optical or acoustic phonons that are involved:

- Raman scattering. This is inelastic light scattering from optical phonons.
- Brillouin scattering. This is inelastic light scattering from acoustic phonons.

The physics of the two processes is essentially the same, but the experimental techniques differ. We will thus consider the general principles first, and then consider the details of each technique separately.

10.5.1 General principles of inelastic light scattering

Inelastic light scattering can be subdivided into two generic types:

- Stokes scattering;
- Anti-Stokes scattering.

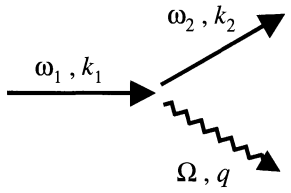

Fig. 10.9 An inelastic light scattering process. The straight arrows represent photons, while the wiggly arrow represents the phonon. The process shown corresponds to Stokes scattering in which the photon is shifted to lower frequency.

Stokes scattering corresponds to the emission of a phonon (or some other type of material excitation), while anti-Stokes scattering corresponds to phonon absorption. The interaction shown in Fig. 10.9 is thus a Stokes process. Conservation of energy during the interaction requires that:

$$\omega_1 = \omega_2 \pm \Omega\,, \tag{10.28}$$

while conservation of momentum gives:

$$\mathbf{k}_1 = \mathbf{k}_2 \pm \mathbf{q}\,. \tag{10.29}$$

The + signs in eqns 10.28 and 10.29 correspond to phonon emission (Stokes scattering), while the − signs correspond to phonon absorption (anti-Stokes scattering). Thus the light is shifted down in frequency during a Stokes process, and up in frequency in an anti-Stokes event.

Anti-Stokes scattering will only be possible if there are phonons present in the material before the light is incident. The probability for anti-Stokes scattering therefore decreases on lowering the temperature as the phonon populations decrease. This means that the probability for anti-Stokes scattering from optical phonons is very low at cryogenic temperatures. On the other hand, Stokes scattering does not require a phonon to be present and can therefore occur at any temperature. The full quantum mechanical treatment shows that the ratio of anti-Stokes to Stokes scattering events is given by:

$$\frac{I_{\text{anti-Stokes}}}{I_{\text{Stokes}}} = \exp\left(-\hbar\Omega/k_{\text{B}}T\right). \tag{10.30}$$

This will be the ratio of the intensities of the anti-Stokes and Stokes lines observed in the Raman or Brillouin spectra.

The frequencies of the phonons involved can be deduced from the frequency shift of the scattered light using eqn 10.28. Thus the main use of inelastic light scattering is to measure phonon frequencies. This means that inelastic light scattering can give complementary information to that obtained from the infrared spectra. For example, infrared reflectivity measurements tell us nothing about the acoustic phonons, but we can measure the frequencies of some of the acoustic modes using Brillouin scattering experiments. We will consider this complementarity in more detail when we discuss the selection rules for Raman scattering in subsection 10.5.2 below.

The maximum phonon frequency in a typical crystal is about $10^{12}-10^{13}$ Hz. This is almost two orders of magnitude smaller than the frequency of a photon in the visible spectral region. Equation 10.28 therefore tells us that the maximum frequency shift for the photon will be around 1 %. The wave vector of the photon is directly proportional to its frequency, and we can therefore make the approximation:

$$|\mathbf{k}_2| \approx |\mathbf{k}_1| = \frac{n\omega}{c}, \tag{10.31}$$

where n is the refractive index of the crystal and ω is the angular frequency of the incoming light.

We know from eqn 10.29 that $|\mathbf{q}| = |\mathbf{k}_1 - \mathbf{k}_2|$. The maximum possible value of $|\mathbf{q}|$ thus occurs for the **back-scattering geometry** in which the outgoing photon is emitted in the direction back towards the source. In this case, we have:

$$q \approx |\mathbf{k} - (-\mathbf{k})| \approx 2\frac{n\omega}{c}. \tag{10.32}$$

By inserting typical values into eqn 10.32, we conclude that the maximum value of q that can be accessed in an inelastic light scattering experiment is of order 10^7 m^{-1}. This is very small compared to the size of the Brillouin zone in a typical crystal ($\sim 10^{10}$ m^{-1}). Inelastic light scattering is thus only able to probe small wave vector phonons.

Raman and Brillouin scattering are generally weak processes, and we therefore expect that the scattering rate will be small. This is because we are dealing with a higher order interaction than for linear interactions such as absorption.

Figure 10.9 shows us that three particles are present in the Feynman diagram for inelastic light scattering rather than the two for absorption (see Fig. 10.1). Therefore, a higher order perturbation term must be involved. This means that we usually have to employ very sensitive detectors to observe the signals even when using a powerful laser beam as the excitation source.

10.5.2 Raman scattering

C.V. Raman was awarded the Nobel prize in 1930 for his discovery of inelastic light scattering from molecules. The process which now carries his name refers to scattering from high frequency excitations such as the vibrational modes of molecules. In the present context of phonon physics, it refers specifically to inelastic light scattering from optical phonons.

Optical phonons are essentially dispersionless near $q = 0$. We argued above that inelastic light scattering can only probe the phonon modes with $q \approx 0$. Therefore, Raman scattering gives little information about the dispersion of optical phonons, and its main use is to determine the frequencies of the LO and TO modes near the Brillouin zone centre. For example, when Raman techniques are used to measure polariton dispersion curves (see Section 10.3, and especially Fig. 10.7), we are only probing a very small portion of the Brillouin zone near $q = 0$.

The complementarity of infrared reflectivity and inelastic light scattering measurements become more apparent when we consider the selection rules for deciding whether a particular optical phonon is Raman active or not. These rules are not the same as those for determining whether the mode is IR active. The full treatment requires the use of group theory. However, a simple rule can be given for crystals that possess inversion symmetry. In these centrosymmetric crystals, the vibrational modes must either have even or odd parity under inversion. The odd parity modes are IR active, while the even parity modes are Raman active. Thus the Raman active modes are not IR active, and *vice versa*. This is called the rule of mutual exclusion, and is a well-known result in molecular physics. In non-centrosymmetric crystals, some modes may be simultaneously IR and Raman active.

As an example of these rules, we can compare silicon and GaAs. Silicon has the diamond structure with inversion symmetry, while GaAs has the non-centrosymmetric zinc blende structure. The TO modes of silicon are not IR active, but they are Raman active, while the TO modes of GaAs are both Raman and IR active.

The observation of a Raman spectrum requires specialized apparatus to overcome the difficulties that are inherent to the technique. We pointed out above that the signal is relatively weak, which means that we have to use an intense source such as a laser to produce a sizeable scattering rate. However, the frequency shift of the scattered photons is quite small. We thus need to resolve a weak Raman signal which is very close in wavelength to the elastically scattered light from the laser.

Figure 10.10 shows a basic experimental arrangement that can be used to measure Raman spectra. The sample is excited with a suitable laser, and the scattered light is collected and focussed onto the entrance slit of a scanning spectrometer. The number of photons emitted at a particular wavelength is

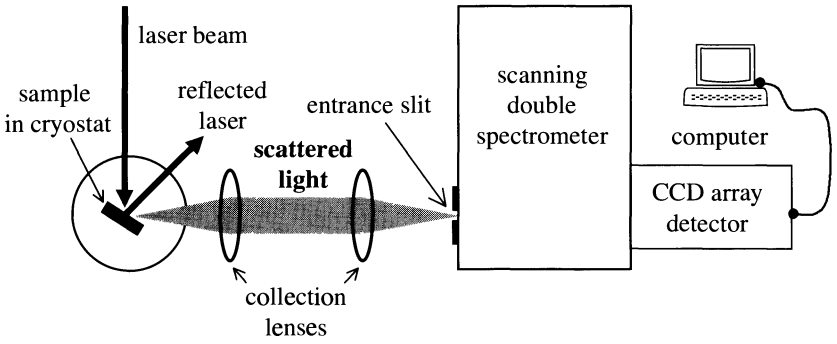

Fig. 10.10 Experimental apparatus used to record Raman spectra. The sample is excited with a laser, and the scattered photons are collected and focussed into a spectrometer. The signals are recorded using a sensitive photon-counting detector such as a photomultiplier tube or a charge coupled device (CCD).

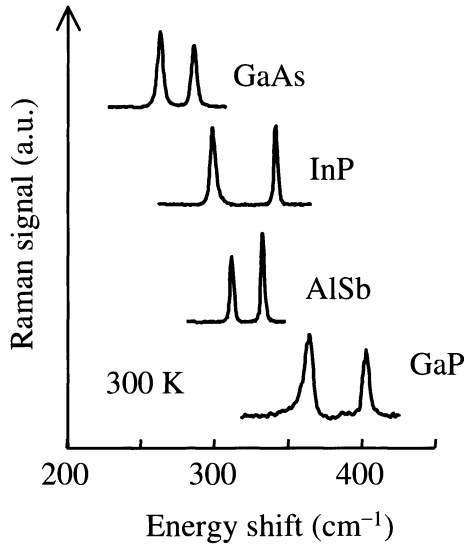

Fig. 10.11 Raman spectra for the TO and LO phonons of GaAs, InP, AlSb and GaP at 300 K using a Nd:YAG laser at 1.06 μm. The spectra are plotted against the wave number shift: 1 cm^{-1} is equivalent to an energy shift of 0.124 meV. The LO mode is the one at higher frequency. After [4], copyright 1972 Excerpta Medica Inc., reprinted with permission.

registered using a photon-counting detector and then the results are stored on a computer for analysis. Photomultiplier tubes have traditionally been employed as the detector in this application, but modern arrangements now tend to use array detectors made with charge coupled devices (CCD arrays). By orientating the sample appropriately, the reflected laser light can be arranged to miss the collection optics. However, this still does not prevent a large number of elastically scattered laser photons entering the spectrometer, and this could potentially saturate the detector. To get around this problem, a high resolution spectrometer with good stray light rejection characteristics is used.

One way to achieve good stray light rejection is to use a double spectrometer, which is essentially two spectrometers in tandem. This both increases the spectral resolution and enhances the rejection of unwanted photons.

Figure 10.11 shows the Raman spectrum obtained from four III–V crystals at 300 K. The laser source was a Nd:YAG laser operating at 1.06 μm, and a double monochromator with a photomultiplier tube were used to detect the signal. Two strong lines are observed for each crystal. These correspond to the Stokes-shifted signals from the TO phonons and LO phonons, with the LO phonons at the higher frequency. The values obtained from this data agree very well with those deduced from infrared reflectivity measurements. (See Exercise 10.13.)

10.5.3 Brillouin scattering

L. Brillouin gave a theoretical discussion of the scattering of light by acoustic waves in 1922. The technique named after him now refers to inelastic light scattering from acoustic phonons. Its main purpose is to determine the dispersion of these acoustic modes.

The frequency shift of the photons in a Brillouin scattering experiment is given by (see Exercise 10.14):

$$\delta\omega = v_s \frac{2n\omega}{c} \sin\frac{\theta}{2}, \tag{10.33}$$

where ω is the angular frequency of the incident light, n is the refractive index of the crystal, v_s is the velocity of the acoustic waves, and θ is the angle through which the light is scattered. Measurements of $\delta\omega$ therefore allow the velocity of the sound waves to be determined if the refractive index is known.

The experimental techniques used for Brillouin scattering are more sophisticated than those for Raman scattering due to the need to be able to detect much smaller frequency shifts. Single-mode lasers must be used to ensure that the laser linewidth is sufficiently small, and a scanning Fabry–Perot interferometer is used instead of a grating spectrometer to obtain the required frequency resolution.

Example 10.2

When light from an argon ion laser operating at 514.5 nm is scattered by optical phonons in a sample of AlAs, two peaks are observed at 524.2 nm and 525.4 nm. What are the values of the TO phonon and LO phonon energies?

Solution

We can work out the energies of the phonons by using eqn 10.28. The photons have been red-shifted, and thus we are dealing with a Stokes process. For the 524.2 nm line we therefore have:

$$\Omega = \omega_1 - \omega_2 = 2\pi c(1/\lambda_1 - 1/\lambda_2) = 6.8 \times 10^{13}\,\text{Hz}.$$

For the 525.4 nm line we find $\Omega = 7.6 \times 10^{13}$ Hz. The higher frequency phonon is the LO mode. Hence we find $\hbar\Omega_{TO} = 45$ meV and $\hbar\Omega_{LO} = 50$ meV.

10.6 Phonon lifetimes

The discussion of the phonon modes as classical oscillators in Section 10.2 led us to introduce a phenomenological damping constant γ. This damping term is needed to explain why the reflectivity in the restrahlen band is less than unity. Analysis of the experimental data led us to conclude that γ is typically in the range 10^{11}–10^{12} s^{-1}. This very rapid damping is a consequence of the finite

lifetime τ of the optical phonons. Since γ is equal to τ^{-1}, the data implies that τ is in the range 1–10 ps.

The very short lifetime of the optical phonons is caused by anharmonicity in the crystal. Phonon modes are solutions of the equations of motion with the assumption that the vibrating atoms are bound in a harmonic potential well. In reality, this is only an approximation that is valid for small displacements. In general, the atoms sit in a potential well of the form:

$$U(x) = C_2x^2 + C_3x^3 + C_4x^4 + \cdots . \tag{10.34}$$

An example of how interatomic interactions lead to a potential of this form is considered in Exercise 10.15.

The term in x^2 in eqn 10.34 is the harmonic term. This leads to simple harmonic oscillator equations of motion with a restoring force $-dU/dx$ proportional to $-x$. The terms in x^3 and higher are the anharmonic terms. These anharmonic terms allow phonon–phonon scattering processes. For example, the term in x^3 allows interactions involving three phonons. Figure 10.12 illustrates two possible permutations for a three-phonon process.

Figure 10.12(a) shows a three-phonon interaction in which one phonon is annihilated and two new phonons are created. This type of anharmonic interaction is responsible for the fast decay of the optical phonons. We can see why this is so by referring to the generic phonon dispersion curve for the first Brillouin zone shown in Fig. 10.13. Lattice absorption or Raman scattering creates optical phonons with $q \approx 0$. Three-phonon processes allow these phonons to decay into two acoustic phonons as indicated in Fig. 10.13. Momentum and energy can be conserved if the two acoustic phonons have opposite wave vectors, and their frequency is half that of the optical phonon. With more complex dispersion relationships, and also the possibility for higher order processes, many other types of decay can contribute to the short lifetime of the optical phonons.

The lifetime of the optical phonons can be deduced from Raman data in two different ways. Firstly, the spectral width of the Raman line is affected by lifetime broadening. Provided that other sources of broadening are smaller, the linewidth in frequency units is expected to be $(2\pi\tau)^{-1}$. Thus measurements of

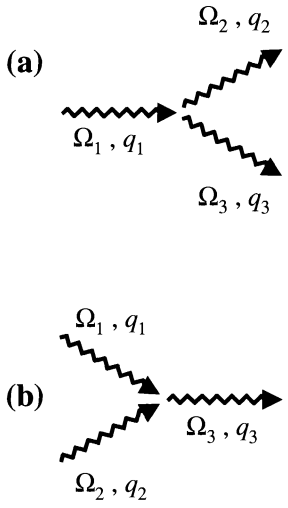

Fig. 10.12 Three phonon interaction processes. Each wiggly arrow represents a phonon. These processes are caused by anharmonicity in the crystal.

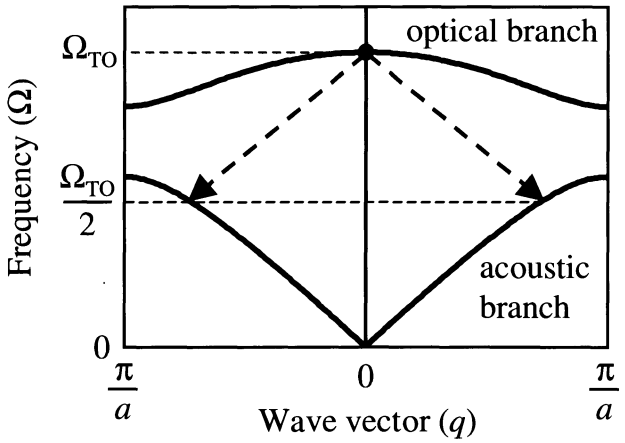

Fig. 10.13 Decay of an optical phonon into two acoustic phonons by a three-phonon interaction of the type shown in Fig. 10.12(a).

the linewidth give a value for τ independently of the reflectivity data. Secondly, τ can be measured directly by time-resolved Raman spectroscopy using short pulse lasers. The lifetime of the LO phonons in GaAs has been determined in this way to be 7 ps at 77 K. This value agrees with the linewidth measured in the conventional Raman spectrum. It is also similar to the lifetime of the TO phonons deduced from reflectivity measurements.

Chapter summary

- The TO phonon modes of polar solids couple strongly to photons when their frequencies and wave vectors match. Acoustic phonons and LO phonons do not couple directly to light waves.
- The interaction between the light and the TO phonon can be modelled by using the classical oscillator model. This model explains why the reflectivity of a polar solid is very high for frequencies in the restrahlen band between ν_{TO} and ν_{LO}.
- The reflectivity in the restrahlen band is 100 % for an undamped system, but damping due to the finite phonon lifetime reduces the reflectivity in real crystals.
- The frequencies of the TO and LO phonon modes are related to each other by the Lyddane–Sachs–Teller relationship given in eqn 10.15.
- The lattice absorbs strongly at the TO phonon frequency. The absorption can be measured directly in thin film samples.
- The strongly coupled phonon–photon waves at frequencies near the restrahlen band are described as polariton modes.
- The electron–phonon coupling in polar crystals leads to polaron effects. Polarons are charge carriers surrounded by a local lattice distortion. The phonon cloud around the electron or hole increases its mass. Polaronic effects are strong in ionic crystals like the alkali halides.
- Raman and Brillouin scattering are inelastic light scattering processes from optical and acoustic phonons respectively. Energy and momentum must be conserved in the scattering process.
- Stokes and anti-Stokes inelastic light scattering processes correspond to phonon emission and absorption respectively. Anti-Stokes scattering from optical phonons is very improbable at low temperatures.
- Optical phonons have short lifetimes due to the possibility of decay into two acoustic phonons by anharmonic interactions.

Further reading

Introductory reading on phonons may be found in practically any solid state physics text, for example: Ashcroft and Mermin (1976), Burns (1985), Ibach and Luth (1995) or Kittel (1996).

The theory of polaritons and polarons is described in more detail in Madelung (1978). Pidgeon (1980) and Seeger (1997) discuss cyclotron resonance experiments in detail. The properties of self-trapped excitons are covered by Song and Williams (1993), while Pope and Swenberg (1999) discuss polaronic hopping transport, especially in organic semiconductors.

A classic text on the infrared physics of molecules and solids is Houghton and Smith (1966). The techniques of inelastic light scattering are described in detail by Mooradian (1972) or Yu and Cardona (1996). The study of phonon dynamics by ultra-fast laser techniques is described by Shah (1999).

References

[1] Madelung, O. (1996). *Semiconductors, basic data*, (2nd edn). Springer-Verlag, Berlin.

[2] Hass, M. (1967). In *Semiconductors and Semimetals, Vol. 3: Optical properties of III–V compounds* (ed. R.K. Willardson and A.C. Beer). Academic Press, New York, p. 3.

[3] Henry, C.H. and Hopfield, J.J. (1965). *Phys. Rev. Lett.*, **15**, 964.

[4] Mooradian, A. (1972). In *Laser Handbook*, Vol. II (ed. F.T. Arecchi and E.O. Schulz-duBois). North Holland, Amsterdam, p. 1409.

[5] Turner, W.J. and Reese, W.E. (1962). *Phys. Rev.*, **127**, 126.

Exercises

(10.1) State, with reasons, which of the following solids would be expected to show strong infrared absorption: (a) ice, (b) germanium, (c) solid argon at 4 K, (d) ZnSe, (e) SiC.

(10.2) Show that the reflectivity of an undamped polar solid falls to zero at a frequency given by

$$\nu = \left(\frac{\epsilon_{st} - 1}{\epsilon_\infty - 1}\right)^{\frac{1}{2}} \nu_{TO},$$

where ϵ_{st} and ϵ_∞ are the low and high frequency dielectric constants, and ν_{TO} is the frequency of the TO phonon mode at the Brillouin zone centre.

(10.3) The static and high frequency dielectric constants of LiF are $\epsilon_{st} = 8.9$ and $\epsilon_\infty = 1.9$ respectively, and the TO phonon frequency ν_{TO} is 9.2 THz. Calculate the upper and lower wavelengths of the restrahlen band.

(10.4) Estimate the reflectivity in the middle of the restrahlen band for a crystal with $\nu_{TO} = 10$ THz, $\epsilon_{st} = 12.1$, and $\epsilon_\infty = 10$, when the damping constant γ is (a) 10^{11} s^{-1} and (b) 10^{12} s^{-1}.

(10.5) Figure 10.14 shows the measured infrared reflectivity of AlSb crystals. Use this data to estimate:

(i) the frequencies of the TO and LO phonons of AlSb near the Brillouin zone centre;

(ii) the static and high frequency dielectric constants, ϵ_{st} and ϵ_∞;

(iii) the lifetime of the TO phonons.

Are the experimental values found in parts (i) and (ii) consistent with the Lyddane–Sachs–Teller relationship?

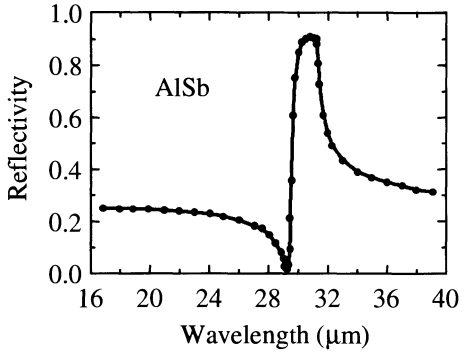

Fig. 10.14 Infrared reflectivity of AlSb. After [5], copyright 1962 American Institute of Physics, reprinted with permission.

(10.6) Estimate the absorption coefficient at the TO phonon frequency in a typical polar solid with a damping constant γ of (a) 10^{11} s^{-1} and (b) 10^{12} s^{-1}. Take $\nu_{TO} = 10$ THz, $\epsilon_{st} = 12.1$, and $\epsilon_\infty = 10$.

(10.7) Explain qualitatively why the reflectivity of NaCl in the middle of the restrahlen band is observed to decrease from 98 % at 100 K to 90 % at 300 K.

(10.8) The static and high frequency dielectric constants of InP are $\epsilon_{st} = 12.5$ and $\epsilon_\infty = 9.6$ respectively, and the TO phonon frequency ν_{TO} is 9.2 THz. Calculate the wave vector of a polariton mode with a frequency of 8 THz. (Ignore phonon damping.)

(10.9) In an infrared absorption experiment on n-type CdTe, the cyclotron resonance condition is satisfied at 3.4 T for the 306 μm line from a deuterated methanol laser. Calculate (i) the polaron mass, and (ii) the rigid lattice electron effective mass, given that $\epsilon_\infty = 7.1$, $\epsilon_{st} = 10.2$, and $\Omega_{LO} = 31.9$ THz.

(10.10) Discuss the qualitative differences you would expect between the Raman spectrum observed from diamond to that shown for the III–V crystals in Fig. 10.11.

(10.11) In an inelastic light scattering experiment on silicon using an argon ion laser at 514.5 nm, Raman peaks are observed at 501.2 nm and 528.6 nm. Account for the origin of the two peaks, and estimate their intensity ratios if the sample temperature is 300 K.

(10.12) NaCl is a centrosymmetric crystal. Would you expect the TO phonon modes to be IR active, or Raman active, or both?

(10.13) Use the data in Fig. 10.11 to deduce the energies in meV of the TO and LO phonons of GaAs, InP, AlSb, and GaP at 300 K. How do the values for GaAs obtained from this data relate to the infrared reflectivity data given in Fig. 10.5 ?

(10.14) A photon of angular frequency ω is scattered inelastically through an angle θ by an acoustic phonon of angular frequency Ω. By considering the conservation of momentum in the process, show that Ω is given by:

$$\Omega = v_s \frac{2n\omega}{c} \sin\frac{\theta}{2},$$

where v_s and n are the velocity of sound and the refractive index in the medium respectively. (You may assume that $\omega \gg \Omega$.) Hence justify eqn 10.33.

A Brillouin scattering experiment is carried out on a crystal with a refractive index of 3 using light from a laser with a wavelength of 488 nm. The scattered photons are found to be down-shifted in frequency by 10 GHz when observed in the back-scattering geometry with $\theta = 180°$. Calculate the speed of sound in the crystal.

(10.15)* The potential energy per molecule of an ionic crystal with a nearest neighbour separation of r may be approximated by the following form:

$$U(r) = \frac{\beta}{r^{12}} - \frac{\alpha e^2}{4\pi\epsilon_0 r},$$

where α is the Madelung constant of the crystal, and β is a fitting parameter.

(i) Account for the functional form of $U(r)$.

(ii) Show that $U(r)$ has a minimum value when $r = r_0$, where $r_0^{11} = 48\beta\pi\epsilon_0/\alpha e^2$.

(iii) Expand U(r) as a Taylor series about r_0, and hence show that the potential takes the form given by eqn 10.34 for small displacements about r_0, stating the value of the constant C_3 in terms of α and r_0.

(10.16) High resolution Raman experiments on a GaAs crystal indicate that the LO phonon line has a spectral width of 0.85 cm^{-1}. Use this value to estimate the lifetime of the LO phonons, on the assumption that the spectrum is lifetime-broadened.

* Exercises marked with an asterisk are more challenging.